Adaptive Modal Identification for Flutter Suppression Control

Nhan T. Nguyen *
NASA Ames Research Center, Moffett Field, CA 94035
Michael Drew †
Stinger Ghaffarian Technologies, Inc., Moffett Field, CA 94035
Sean S. Swei ‡
NASA Ames Research Center, Moffett Field, CA 94035

In this paper, we will develop an adaptive modal identification method for identifying the frequencies and damping of a flutter mode based on model-reference adaptive control (MRAC) and least-squares methods. The least-squares parameter estimation will achieve parameter convergence in the presence of persistent excitation whereas the MRAC parameter estimation does not guarantee parameter convergence. Two adaptive flutter suppression control approaches are developed: one based on MRAC and the other based on the least-squares method. The MRAC flutter suppression control is designed as an integral part of the parameter estimation where the feedback signal is used to estimate the modal information. On the other hand, the separation principle of control and estimation is applied to the least-squares method. The least-squares modal identification is used to perform parameter estimation.

I. Introduction

There has been increasing research interest in wing shaping control technology in recent years. This is in response to the need for energy-efficient aircraft design that employs light-weight materials for aircraft structures. Reducing airframe operational empty weight (OEW) using advanced composite materials is one of the major design considerations for improving energy efficiency. As a result, aircraft wing structures in modern transport aircraft have become much more flexible than older-generation aircraft wings. In some modern transport aircraft, the wing flexibility can be double that of an older-generation transport aircraft. As structural flexibility increases, aeroelastic interactions with aerodynamic forces and moments can potentially degrade aerodynamic efficiency and compromise vehicle stability and control. One consequence of increased wing flexibility is a reduced flutter margin. Transport aircraft are designed to meet FAA certification for flutter clearance.

Wing shaping control concepts for drag reduction are being studied by NASA to leverage wing flexibility for aerodynamic performance.[1,2] By re-twisting a flexible wing and using variable camber aerodynamic control surfaces, aircraft wings can have a mission-adaptive capability.[3] In recognition of the role of aeroelasticity on aircraft performance and dynamics, NASA Advanced Air Transport Technology (AATT) project is conducting research in the area of Performance Adaptive Aeroelastic Wing (PAAW). This research develops concepts such as the variable camber continuous trailing edge flap (VCCTEF) to enable wing shaping control for aerodynamic performance and dynamics.[4]

Structural dynamic interactions with aerodynamics alter natural frequencies and damping of flight structures that give rise to flutter.[5] Flutter is a dynamic stability problem caused by non-conservative work done by aerodynamic forces on flight structures. Active flutter suppression control is required to suppress any unstable flutter modes that may appear below the flutter clearance speed of an aircraft. Flutter can be

*NASA Ames Research Center, Research Scientist, AIAA Associate Fellow, nhan.t.nguyen@nasa.gov
†Stinger Ghaffarian Technologies Inc., NASA Ames Research Center, Research Engineer, michael.c.drew@nasa.gov
‡NASA Ames Research Center, Research Scientist, sean.s.swei@nasa.gov

modeled by a second-order system with parameter-varying frequencies and damping.[6] Often times, these parameter-varying frequencies and damping are not known accurately due to complex aeroelastic interactions. Real-time modal identification can potentially helps to determine the unknown parameters of the aeroelastic model of an aircraft. The information obtained from the modal identification can be used to devise an active flutter control to improve the flutter margin.

In this paper, we will develop an adaptive modal identification method for identifying the frequencies and damping of a flutter mode based on model-reference adaptive control (MRAC) and least-squares methods. The least-squares parameter estimation will achieve parameter convergence in the presence of persistent excitation whereas the MRAC parameter estimation does not guarantee parameter convergence.[7] The separation principle of control and estimation can be applied to the least-squares method. The least-squares modal identification is used to perform parameter estimation. Then, an adaptive flutter suppression control could be designed using the parameter estimates obtained from the least-squares modal identification. The least-squares parameter estimation method is demonstrated on an airfoil flutter problem. The recursive least-squares approach is observed to be highly effective in achieving parameter convergence.

II. Flutter Model

The aeroelastic equation that describes flutter of an aircraft wing is given by

$$M\ddot{q} + C\dot{q} + Kq = Q \tag{1}$$

where $q \in \mathbb{R}^n$ is the generalized coordinate vector, $M \in \mathbb{R}^{n\times n}$ is the generalized mass matrix, $C \in \mathbb{R}^{n\times n}$ is the generalized damping matrix, $K \in \mathbb{R}^{n\times n}$ is the generalized stiffness matrix, and $Q \in \mathbb{R}^n$ is the generalized aerodynamic force vector.

The generalized aerodynamic force vector Q is a complex function of the aerodynamic characteristics, the so-called reduced frequency, the generalized displacement q, the generalized velocity $\dot{q}$, the generalized acceleration $\ddot{q}$, the control surface deflection $\delta \in \mathbb{R}^m$ which comprises m control surfaces, the deflection rate $\dot{\delta}$, and the deflection acceleration $\ddot{\delta}$. So, in general, it can be expressed as

$$\begin{aligned} Q = Q_{\ddot{q}}\left(\rho_\infty, V_\infty\right)\ddot{q} + Q_{\dot{q}}\left(\rho_\infty, V_\infty, k\right)\dot{q} + Q_q\left(\rho_\infty, V_\infty, k\right)q + Q_{\ddot{\delta}}\left(\rho_\infty, V_\infty\right)\ddot{\delta} \\ + Q_{\dot{\delta}}\left(\rho_\infty, V_\infty, k\right)\dot{\delta} + Q_\delta\left(\rho_\infty, V_\infty, k\right)\delta \end{aligned} \tag{2}$$

where $k = \frac{\omega\bar{c}}{2V_\infty}$ is the reduced frequency, ω is the flutter frequency, $\bar{c}$ is the mean aerodynamic chord, V_∞ is the airspeed, and ρ_∞ is the air density which is a function of altitude.

The generalized coordinate of a flutter mode can be described by $q_f(t) = q_{0_f}e^{(-\zeta\omega+i\omega)t}$ where ζ is the modal damping. Flutter occurs when the damping of a flutter mode crosses zero from $\zeta > 0$ to $\zeta < 0$. Let $q = \begin{bmatrix} q_f & q_s \end{bmatrix}^\top$ where $q_f \in \mathbb{R}$ is the generalized coordinate of the flutter mode and $q_s \in \mathbb{R}^{n-1}$ is the generalized coordinate vector of the remaining modes.

The aeroelastic equation for the flutter mode can be separated from Eq. (1) as

$$\begin{aligned} \left(M_f - Q_{f\ddot{q}_f}\right)\ddot{q}_f + \left(C_f - Q_{f\dot{q}_f}\right)\dot{q}_f + \left(K_f - Q_{fq_f}\right)q_f = \left(Q_{f\ddot{q}_s} - M_{fs}\right)\ddot{q}_s + \left(Q_{f\dot{q}_s} - C_{fs}\right)\dot{q}_s \\ + \left(Q_{fq_s} - K_{fs}\right)q_s + Q_{f\ddot{\delta}}\ddot{\delta} + Q_{f\dot{\delta}}\dot{\delta} + Q_{f\delta}\delta \end{aligned} \tag{3}$$

$$\begin{aligned} \left(M_s - S_{s\ddot{q}_s}\right)\ddot{q}_s + \left(C_s - Q_{s\dot{q}_s}\right)\dot{q}_s + \left(K_s - Q_{sq_s}\right)q_s = \left(Q_{s\ddot{q}_f} - M_{sf}\right)\ddot{q}_f + \left(Q_{s\dot{q}_f} - C_{sf}\right)\dot{q}_f \\ + \left(Q_{sq_f} - K_{sf}\right)q_f + Q_{s\ddot{\delta}}\ddot{\delta} + Q_{s\dot{\delta}}\dot{\delta} + Q_{s\delta}\delta \end{aligned} \tag{4}$$

Let $\omega_f^2 = \frac{K_f - Q_{fq_f}}{M_f - Q_{f\ddot{q}_f}}$ and $2\zeta_f\omega_f = \frac{C_f - Q_{f\dot{q}_f}}{M_f - Q_{f\ddot{q}_f}}$. Suppose the control surface deflection is commanded by $\delta = \delta_0 e^{i\omega t}$ where $\omega = \omega_f + \epsilon$ is the excitation frequency with ϵ as a small number. The response of the generalized coordinate of the flutter mode is described by $q_f = q_{0_f}e^{i(\omega t-\phi)}$ where ϕ is a phase lag, while the response of the generalized coordinates of the remaining modes is described by $q_s = q_{0_s}e^{i(\omega t-\psi)}$ where ψ is the phase lag. Then the responseq_s is obtained as

$$q_s = F^{-1}Gq_f + H^{-1}\delta \tag{5}$$

where $F = -\left(M_s - S_{s\ddot{q}_s}\right)\omega^2 + \left(C_s - Q_{s\dot{q}_s}\right)i\omega + \left(K_s - Q_{sq_s}\right)$, $G = -\left(Q_{s\ddot{q}_f} - M_{sf}\right)\omega^2 + \left(Q_{s\dot{q}_f} - C_{sf}\right)i\omega + \left(Q_{sq_f} - K_{sf}\right)$, and $H = -Q_{s\ddot{\delta}}\omega^2 + Q_{s\dot{\delta}}i\omega + Q_{s\delta}$.

The response of the flutter mode is computed to be

$$q_f = \frac{\left[-\left(Q_{f\ddot{q}_s} - M_{fs}\right)\omega^2 + \left(Q_{f\dot{q}_s} - C_{fs}\right)i\omega + \left(Q_{fq_s} - K_{fs}\right)\right]\left(F^{-1}Gq_f + H^{-1}\delta\right)}{\left(M_f - Q_{f\ddot{q}_f}\right)\left(-\omega^2 + 2\zeta_f\omega_f i\omega + \omega_f^2\right)} + \frac{\left(-Q_{f\ddot{\delta}}\omega^2 + Q_{f\dot{\delta}}i\omega + Q_{f\delta}\right)\delta}{\left(M_f - Q_{f\ddot{q}_f}\right)\left(-\omega^2 + 2\zeta_f\omega_f i\omega + \omega_f^2\right)} \quad (6)$$

Since $\omega = \omega_f + \epsilon$, $\zeta \to 0$ as $\epsilon \to 0$. Therefore, the amplitude of q_f is larger than that of q_s. Thus, the flutter mode is the most dominant response in the presence of persistent excitation input from δ. Therefore, it can be expressed as

$$\ddot{q}_f + 2\zeta_f\omega_f\dot{q}_f + \omega_f^2 q_f = b_1\ddot{\delta} + b_2\dot{\delta} + b_3\delta + \Delta_q \quad (7)$$

where Δ_q is an unmodeled dynamic due to the remaining modes.

Suppose the measurement is an acceleration of the wing bending deflection at a given location z. Then, the acceleration is expressed in terms of the generalized coordinates as

$$\ddot{w} = \Phi(z)\,\ddot{q} = \phi_f(z)\,\ddot{q}_f + \Phi_s(y)\,\ddot{q}_s \quad (8)$$

where $\Phi(z) = \begin{bmatrix} \phi_f(z) & \Phi_s(z) \end{bmatrix} \in \mathbb{R}^n$ is the mode shape vector, $\phi_f(z) \in \mathbb{R}$ is the mode shape at the measurement location for the flutter mode, and $\Phi_s(z) \in \mathbb{R}^{n-1}$ is the mode shape vector for the remanning modes.

When the excitation frequency approaches the flutter frequency, the acceleration response is predominantly due to $\ddot{q}_f$. Thus the acceleration can be written as

$$\ddot{w} = \phi_f(z)\,\ddot{q}_f + \Delta_w \quad (9)$$

where Δ_w is the contribution of the remaining modes to the acceleration measurements which is assumed to be small.

Therefore, the measurement equation is approximated as

$$\ddot{w} + 2\zeta_f\omega_f\dot{w} + \omega_f^2 w = c_1\ddot{\delta} + c_2\dot{\delta} + c_3\delta + \Delta_q \quad (10)$$

where $c_i = \phi_f(z)\,b_i$, $i = 1, 2, 3$.

We will use this equation to estimate the fluter frequency and damping. Then, using this information, an adaptive control can be designed to suppress the flutter mode.

Example: Consider an airfoil in pitch and plunge as shown in Fig. 1.

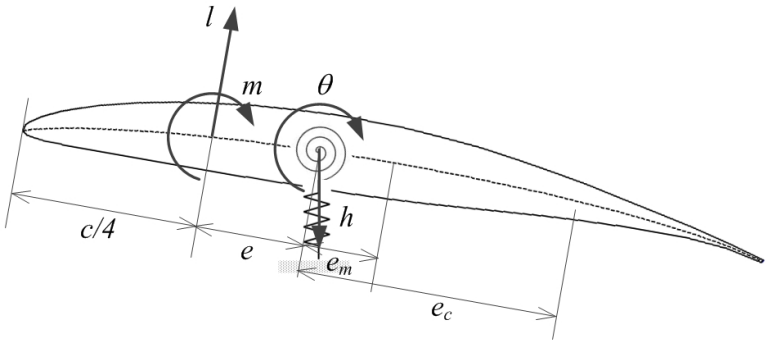

Figure 1. Airfoil in Pitch and Plunge

Consider a quasi-static flutter problem whereby we neglect the aerodynamic mass and damping matrices. The equations of motion are written as

$$\begin{bmatrix} m & me_{cg} \\ me_{cg} & I \end{bmatrix} \begin{bmatrix} \ddot{h} \\ \ddot{\theta} \end{bmatrix} + \begin{bmatrix} 2\zeta_n\sqrt{mk_h} & \frac{G(k)}{k}\frac{c_{l_\alpha} q_\infty c^2}{2V_\infty} \\ 0 & 2\zeta_\theta\sqrt{k_\theta I} - \frac{G(k)}{k}\frac{c_{l_\alpha} q_\infty c^2 e}{2V_\infty} \end{bmatrix} \begin{bmatrix} \dot{h} \\ \dot{\theta} \end{bmatrix}$$
$$+ \begin{bmatrix} k_h & F(k)\, c_{l_\alpha} q_\infty c \\ 0 & k_\theta - F(k)\, c_{l_\alpha} q_\infty ce \end{bmatrix} \begin{bmatrix} h \\ \theta \end{bmatrix} = \begin{bmatrix} -F(k)\, c_{l_\delta} q_\infty c \\ F(k)\left(c_{m_\delta} + \frac{e}{c} c_{l_\delta}\right) q_\infty c^2 \end{bmatrix} \delta + \begin{bmatrix} -\frac{G(k)}{k}\frac{c_{l_\delta} q_\infty c^2}{2V_\infty} \\ \frac{G(k)}{k}\frac{\left(c_{m_\delta} + \frac{e}{c} c_{l_\delta}\right) q_\infty c^3}{2V_\infty} \end{bmatrix} \dot{\delta}$$

Given $m = 1.86733$ slug/ft, $I = 15.5611$ slug-ft, $k_h = 500$ lb/ft^2, $k_\theta = 10,000$ lb, $\zeta_h = \zeta_\theta = 0.01$, $c = 10$ ft, $e = 0.15c$, $e_{cg} = 0.1c$, $c_{l_\alpha} = \frac{2\pi}{\sqrt{1-M_\infty^2}}$ for subsonic flow, $M_\infty = 0.4$, and $\rho_\infty = 2.37756 \times 10^{-3}$ slug/ft^3 at standard sea level. The control derivatives are given by

$$c_{l_\delta} = \frac{c_{l_\alpha}}{\pi}\left[\cos^{-1}\left(1 - 2\frac{c_f}{c}\right) + 2\sqrt{\frac{c_f}{c}\left(1 - \frac{c_f}{c}\right)}\right] \tag{11}$$

$$c_{m_\delta} = -\frac{c_{l_\alpha}}{2\pi}\left[\cos^{-1}\left(1 - 2\frac{c_f}{c}\right) + 2\left(2 - \frac{c_f}{c}\right)\sqrt{\frac{c_f}{c}\left(1 - \frac{c_f}{c}\right)}\right] \tag{12}$$

where $c_f = 2$ ft is the flap chord.

Figures 2 and 3 show the frequencies and damping of the pitch and plunge as a function of the equivalent airspeed in knots (KEAS). The flutter mode corresponds to the plunge mode which occurs at an airspeed of 61.7353 knots and a frequency of 16.2804 rad/sec. The damping plot actually shows the structural damping required to achieve neutral stability. It is two times the negative value of the viscous damping ratio.

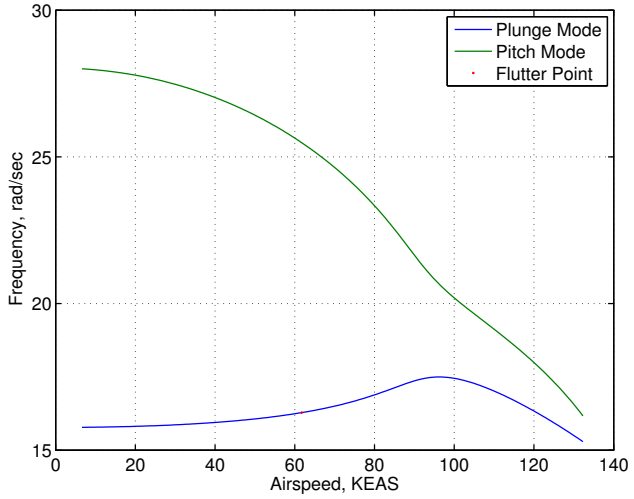

Figure 2. Frequencies of Airfoil in Pitch and Plunge

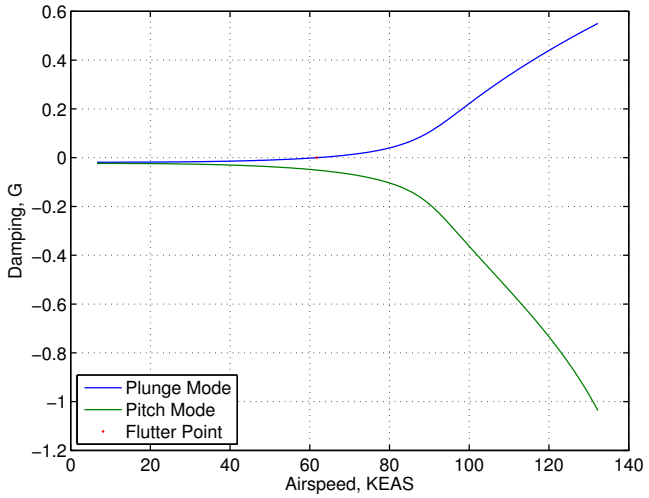

Figure 3. Damping of Airfoil in Pitch and Plunge

III. Parameter Estimation of Second-Order System

Consider a second-order system with matched uncertainty in a state-space form

$$\dot{x} = Ax + B\left[u + \Theta^{*\top}\Phi\left(x\right)\right] \tag{13}$$

where A and B unknown but sign of b is known.

Assuming that there exist K_x and k_r that satisfy the model matching conditions, and furthermore that A_m and B_m also correspond to a second-order system. Then A and B can be identified. Let

$$A = \begin{bmatrix} 0 & 1 \\ -\omega_n^2 & -2\zeta\omega_n \end{bmatrix},\ B = \begin{bmatrix} 0 \\ b \end{bmatrix},\ A_m = \begin{bmatrix} 0 & 1 \\ -\omega_m^2 & -2\zeta_m\omega_m \end{bmatrix},\ B = \begin{bmatrix} 0 \\ b_m \end{bmatrix} \tag{14}$$

The model matching conditions are

$$\hat{A}\left(t\right) + \hat{B}\left(t\right)K_x\left(t\right) = A_m \tag{15}$$

$$\hat{B}\left(t\right)k_r\left(t\right) = B_m \tag{16}$$

from which K_x and k_r are determined by

$$K_x = \left(\hat{B}^\top\hat{B}\right)^{-1}\hat{B}^\top\left(A_m - \hat{A}\right) = \frac{1}{\hat{b}^2}\begin{bmatrix} 0 & \hat{b} \end{bmatrix}\begin{bmatrix} 0 & 0 \\ -\omega_m^2 + \hat{\omega}_n^2 & -2\zeta_m\omega_m + 2\hat{\zeta}\hat{\omega}_n \end{bmatrix}$$
$$= \frac{1}{\hat{b}}\begin{bmatrix} -\omega_m^2 + \hat{\omega}_n^2 & -2\zeta_m\omega_m + 2\hat{\zeta}\hat{\omega}_n \end{bmatrix} \tag{17}$$

$$k_r = \left(\hat{B}^\top\hat{B}\right)^{-1}\hat{B}^\top B_m = \frac{1}{\hat{b}^2}\begin{bmatrix} 0 & \hat{b} \end{bmatrix}\begin{bmatrix} 0 \\ b_m \end{bmatrix} = \frac{b_m}{\hat{b}} \tag{18}$$

where $\hat{A}$, $\hat{B}$, $\hat{\omega}_n$, and $\hat{\zeta}$ are estimates of A, B, ω_n, and ζ, respectively.

Let $\tilde{A}\left(t\right) = \hat{A}\left(t\right) - A$ and $\tilde{B}\left(t\right) = \hat{B}\left(t\right) - B$ be the parameter estimation errors. Now rewriting the plant model as

$$\dot{x} = \left(\hat{A} - \tilde{A}\right)x + \left(\hat{B} - \tilde{B}\right)\left[u + \Theta^{*\top}\Phi\left(x\right)\right] \tag{19}$$

The adaptive control is designed as

$$u = K_x\left(t\right)x + k_r\left(t\right)r - \Theta^\top\left(t\right)\Phi\left(x\right) \tag{20}$$

Then, substituting Eqs. (15), (40), and (17) into Eq. (18) yields

$$\dot{x} = \left(\hat{A} - \tilde{A}\right) x + \hat{B}\left[K_x x + k_r r - \Theta^\top \Phi(x) + \Theta^{*\top} \Phi(x)\right] - \tilde{B}\left[K_x x + k_r r - \Theta^\top \Phi(x) + \Theta^{*\top} \Phi(x)\right]$$
$$= \left(\underbrace{\hat{A} + \hat{B} K_x}_{A_m} - \tilde{A}\right) x + \underbrace{\hat{B} k_r}_{B_m} r - B\tilde{\Theta}^\top \Phi(x) - \tilde{B}\left(K_x x + k_r r\right) \quad (21)$$

where $\tilde{\Theta}(t) = \Theta(t) - \Theta^*$ is the matched uncertain parameter estimation error.

Then, the tracking error equation is established as

$$\dot{e} = \dot{x}_m - \dot{x} = A_m e + \tilde{A} x + \tilde{B}\bar{u} + B\tilde{\Theta}^\top \Phi(x) \quad (22)$$

where $\bar{u} = K_x(t)\, x + k_r(t)\, r$.

Choose a Lyapunov candidate function

$$V\left(e, \tilde{A}, \tilde{B}, \tilde{\Theta}\right) = e^\top P e + \text{trace}\left(\tilde{A}\Gamma_A^{-1}\tilde{A}^\top\right) + \frac{\tilde{B}^\top \tilde{B}}{\gamma_b} + |b|\,\tilde{\Theta}^\top \Gamma_\Theta^{-1}\tilde{\Theta} \quad (23)$$

where $\Gamma_A = \Gamma_A^\top > 0$ and $\Gamma_\Theta = \Gamma_\Theta^\top > 0$ are positive definite adaptation rate matrices.

$\dot{V}\left(e, \tilde{A}, \tilde{B}, \tilde{\Theta}\right)$ is evaluated as

$$\dot{V}\left(e, \tilde{A}, \tilde{B}, \tilde{\Theta}\right) = -e^\top Q e + 2e^\top P\left[\tilde{A}x + \tilde{B}\bar{u} + B\tilde{\Theta}^\top \Phi(x)\right] + \text{trace}\left(2\tilde{A}\Gamma_A^{-1}\dot{\tilde{A}}^\top\right) + \frac{2\tilde{B}^\top \dot{\tilde{B}}}{\gamma_b} + 2|b|\,\tilde{\Theta}^\top \Gamma_\Theta^{-1}\dot{\tilde{\Theta}} \quad (24)$$

The following parameter estimation adaptive laws are then obtained

$$\dot{\tilde{A}}^\top = -\Gamma_A x e^\top P \quad (25)$$

$$\dot{\tilde{B}} = -\gamma_b P e \bar{u} \quad (26)$$

$$\dot{\Theta} = -\Gamma_\Theta \Phi(x)\, e^\top \bar{P}\,\text{sgn}(b) \quad (27)$$

where $\bar{P} = \frac{PB}{b}$.

It follows that $e(t)$, $\tilde{A}(t)$, $\tilde{B}(t)$, and $\tilde{\Theta}(t)$ are bounded since

$$\dot{V}\left(e, \tilde{A}, \tilde{B}, \tilde{\Theta}\right) = -e^\top Q e \le -\lambda_{min}(Q)\,\|e\|^2 \quad (28)$$

$V\left(e, \tilde{A}, \tilde{B}, \tilde{\Theta}\right)$ has a finite limit as $t \to \infty$ since

$$V(t \to \infty) = V(t_0) - \int_{t_0}^{\infty} \lambda_{min}(Q)\,\|e\|^2\, dt < \infty \quad (29)$$

It can be shown that $\dot{V}\left(e, \tilde{A}, \tilde{B}, \tilde{\Theta}\right)$ is uniformly continuous because $\ddot{V}\left(e, \tilde{A}, \tilde{B}, \tilde{\Theta}\right)$ is bounded. Then, applying the Barbalat's lemma, one can conclude that the tracking error is asymptotically stable with $e(t) \to 0$ as $t \to \infty$. However, this does not imply that the parameter estimation errors $\tilde{A}(t)$, $\tilde{B}(t)$, $\tilde{\Theta}(t)$ tend to zero. So parameter convergence is not guaranteed with MRAC.

■

Let

$$\hat{\tilde{A}} = \begin{bmatrix} 0 & 1 \end{bmatrix} \hat{A} = \begin{bmatrix} 0 & 1 \end{bmatrix} \begin{bmatrix} 0 & 1 \\ -\hat{\omega}_n^2 & -2\hat{\zeta}\hat{\omega}_n \end{bmatrix} = \begin{bmatrix} -\hat{\omega}_n^2 & -2\hat{\zeta}\hat{\omega}_n \end{bmatrix} \quad (30)$$

and since

$$\hat{b} = \begin{bmatrix} 0 & 1 \end{bmatrix} \hat{B} = \begin{bmatrix} 0 & 1 \end{bmatrix} \begin{bmatrix} 0 \\ \hat{b} \end{bmatrix} \quad (31)$$

then the adaptive laws can be expressed in terms of the estimates of the unknown quantities ω_n, ζ, and b as

$$\dot{\hat{A}}^\top = -\Gamma_A x e^\top P \begin{bmatrix} 0 \\ 1 \end{bmatrix} = -\Gamma_A x e^\top \bar{P} \tag{32}$$

$$\dot{\hat{b}} = -\gamma_b \begin{bmatrix} 0 & 1 \end{bmatrix} Peu = -\gamma_b \bar{P}^\top e \bar{u} = -\gamma_b \bar{u} e^\top \bar{P} \tag{33}$$

Let

$$\Gamma_A = \begin{bmatrix} \gamma_\omega & 0 \\ 0 & \gamma_\zeta \end{bmatrix} > 0 \tag{34}$$

Then

$$\frac{d}{dt}\left(-\hat{\omega}_n^2\right) = -\gamma_\omega x_1 e^\top \bar{P} \tag{35}$$

or

$$\dot{\hat{\omega}}_n = \frac{\gamma_\omega x_1 e^\top \bar{P}}{2\hat{\omega}_n} \tag{36}$$

$$\frac{d}{dt}\left(-2\hat{\zeta}\hat{\omega}_n\right) = -2\hat{\omega}_n \dot{\hat{\zeta}} - 2\hat{\zeta}\dot{\hat{\omega}}_n = -\gamma_\zeta x_2 e^\top \bar{P} \tag{37}$$

or

$$\dot{\hat{\zeta}} = \frac{\left(\gamma_\zeta x_2 \hat{\omega}_n - \gamma_\omega x_1 \hat{\zeta}\right) e^\top \bar{P}}{2\hat{\omega}_n^2} \tag{38}$$

To prevent the possibility of $\hat{\omega}_n = 0$ or $\hat{b} = 0$ that will cause the adaptive laws to blow up, both the adaptive laws for estimating $\hat{\omega}_n$ and $\hat{b}$ need to be modified by the projection method as follows:

$$\dot{\hat{\omega}}_n = \begin{cases} \frac{\gamma_\omega x_1 e^\top \bar{P}}{2\hat{\omega}_n} & \text{if } \hat{\omega}_n > \omega_0 > 0 \text{ or if } \hat{\omega}_n = \omega_0 \text{ and } \dot{\hat{\omega}}_n \geq 0 \\ 0 & \text{otherwise} \end{cases} \tag{39}$$

$$\dot{\hat{b}} = \begin{cases} -\gamma_b \bar{u} e^\top \bar{P} & \text{if } \left|\hat{b}\right| > b_0 \text{ or if } \left|\hat{b}\right| = b_0 \text{ and } \frac{d|\hat{b}|}{dt} \geq 0 \\ 0 & \text{otherwise} \end{cases} \tag{40}$$

In the modified adaptive law for $\hat{\omega}_n$, it is assumed that $\hat{\omega}_n$ is always a positive quantity for a physically realizable system.

Example: For the following second-order SISO system

$$\ddot{x}_1 + \zeta\omega_n \dot{x}_1 + \omega_n^2 x_1 = b\left[u + \Theta^{*\top}\Phi(x)\right]$$

where ζ, ω_n, and b are unknown, but $b > 0$ is known, we design an indirect adaptive controller using the following information: $\zeta_m = 0.5$, $\omega_m = 2$, $b_m = 4$, $r(t) = \sin 2t$, and

$$\Phi(x) = \begin{bmatrix} 1 \\ x_1^2 \end{bmatrix}$$

For simulation purpose, the unknown parameters are given to be $\zeta = -0.5$, $\omega_n = 1$, $b = 1$, and $\Theta^{*\top} = \begin{bmatrix} 0.5 & -0.1 \end{bmatrix}$, and all initial conditions are assumed to be zero, except for $\hat{\omega}_n(0) = 0.8$ and $\hat{b}(0) = 0.6$. For simplicity, we use the unmodified adaptive laws for $\hat{\omega}_n$ and $\hat{b}$. Use $\gamma_\omega = \gamma_\zeta = \gamma_b = 10$ and $\Gamma_\Theta = 10I$. Figure 5 shows the closed-loop response of the second-order system to MRAC. All signals are bounded and the tracking error tends to zero asymptotically. Figure 5 shows the parameter convergence which is quite good even though the excitation frequency $\omega = 2$ rad/sec is not too close to the plant frequency $\omega_n = 1$ rad/sec. The adaptive control is able to stabilize the unstable plant.

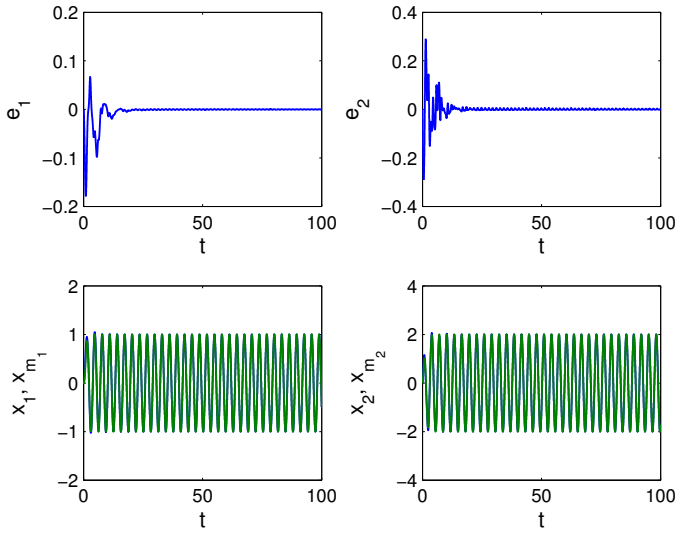

Figure 4. Response to MRAC of Second-Order System

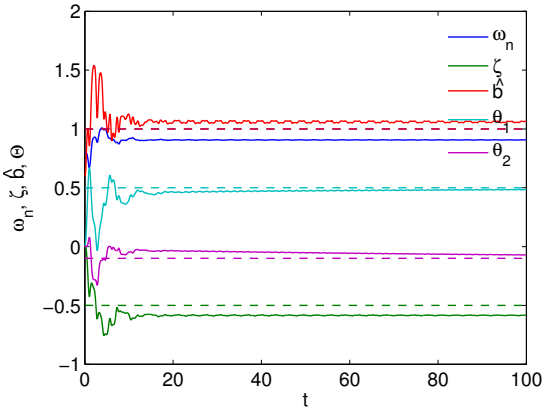

Figure 5. Response to MRAC of Second-Order System

■

Note that the adaptive modal identification based on MRAC assumes zero contribution from the control surface deflection dynamics due to the terms $\dot{\delta}$ and $\ddot{\delta}$. This may be a reasonable assumption if the excitation frequency is small. Increasing the excitation frequency can cause these terms to become significant. In such a case, the dynamics of the control surface deflection must be accounted for. Moreover, we will consider least-squares parameter estimation method which is generally more robust than MRAC and can guarantee parameter convergence if the persistent excitation condition is satisfied.

Going back to the measurement equation (10), we establish an estimator model as

$$\ddot{w}_d + 2\hat{\zeta}\hat{\omega}_f\dot{w} + \hat{\omega}_n^2 w = \hat{c}_1\ddot{\delta} + \hat{c}_2\dot{\delta} + \hat{c}_3\delta \tag{41}$$

The output is the acceleration $\ddot{w}$. We compute the plant modeling error between the true output and the estimated output $\ddot{w}_d$ as follows:

$$\epsilon = \ddot{w}_d - \ddot{w} = -2\tilde{\zeta}\tilde{\omega}_f\dot{w} - \tilde{\omega}_f^2 w + \tilde{c}_1\ddot{\delta} + \tilde{c}_2\dot{\delta} + \tilde{c}_1\delta \tag{42}$$

Note that the system is open-loop with the control surface deflection providing the persistent excitation signal $\delta = \delta_0 e^{i\omega t}$. The parameter estimation will be computed by a least-squares gradient method by

minimizing the cost function $J = \frac{1}{2}\epsilon^2$. Taking the gradients of the cost function with respect to the parameter estimates yields

$$\frac{\partial J}{\partial\left(\tilde{\zeta}\tilde{\omega}_f\right)} = -2\dot{w}\epsilon \tag{43}$$

$$\frac{\partial J}{\partial\left(\tilde{\omega}_f^2\right)} = -w\epsilon \tag{44}$$

$$\frac{\partial J}{\partial \tilde{c}_1} = \ddot{\delta}\epsilon \tag{45}$$

$$\frac{\partial J}{\partial \tilde{c}_2} = \dot{\delta}\epsilon \tag{46}$$

$$\frac{\partial J}{\partial \tilde{c}_3} = \delta\epsilon \tag{47}$$

The least-squares gradient adaptive laws for modal identification are then obtained as

$$\frac{d}{dt}\left(\hat{\omega}_f^2\right) = -\gamma_\omega \frac{\partial J}{\partial\left(\tilde{\omega}_f^2\right)} = \gamma_\omega w\epsilon \tag{48}$$

$$\frac{d}{dt}\left(\hat{\zeta}_f\hat{\omega}_f\right) = -\gamma_\zeta \frac{\partial J}{\partial\left(\tilde{\zeta}\tilde{\omega}_f\right)} = 2\gamma_\zeta \dot{w}\epsilon \tag{49}$$

$$\dot{\hat{c}}_1 = -\gamma_{c_1}\frac{\partial J}{\partial \tilde{c}_1} = -\gamma_{c_1}\ddot{\delta}\epsilon \tag{50}$$

$$\dot{\hat{c}}_2 = -\gamma_{c_2}\frac{\partial J}{\partial \tilde{c}_2} = -\gamma_{c_2}\dot{\delta}\epsilon \tag{51}$$

$$\dot{\hat{c}}_3 = -\gamma_{c_3}\frac{\partial J}{\partial \tilde{c}_3} = -\gamma_{c_2}\delta\epsilon \tag{52}$$

where $\gamma_\omega > 0$, $\gamma_\zeta > 0$, and $\gamma_{c_i} > 0$, $i = 1, 2, 3$ are the adaptation rates.

The frequency estimation adaptive law can also be written as

$$\dot{\hat{\omega}}_f = \frac{\gamma_\omega w\epsilon}{2\hat{\omega}_f} \tag{53}$$

$$\dot{\hat{\zeta}} = \frac{4\gamma_\zeta\hat{\omega}_f\dot{w}\epsilon - \gamma_\omega\hat{\zeta}w\epsilon}{2\hat{\omega}_f^2} \tag{54}$$

In the presence of the persistent excitation conditions $\frac{1}{T}\int_0^T w^2 dt = \|w\|_2^2 > 0$ and $\frac{1}{T}\int_0^T \delta^2 dt = \|\delta\|_2^2 > 0$, exponential parameter convergence will be achieved. Since $\delta = \delta_0 e^{i\omega t}$, then $\|\delta\|_2^2 = \frac{\delta_0^2}{2}$; and $w = w_0 e^{i(\omega t - \phi)}$, then $\|w\|_2^2 = \frac{w_0^2}{2}$. Therefore, the least-squares adaptive modal identification will achieve parameter convergence. Then, in theory, this implies $\hat{\omega}_f(t) \to \omega_f$, $\hat{\zeta}(t) \to \zeta_f$, $\hat{c}_1(t) \to c_1$, $\hat{c}_2(t) \to c_2$, and $\hat{c}_3(t) \to c_3$ in the limit as $t \to \infty$. However, in practice, the parameter convergence is only approximate because the estimator model does not represent the true plant. The modal contribution of those modes not captured in the estimator model will influence the parameter convergence.

Adaptive flutter suppression control can be designed based on the parameter estimation. We assume a time-varying feedback law $\delta(t) = k_w(t)\, w(t) + r(t)$, where $k_w(t)$ is an adaptive feedback gain and $r(t)$ is a command signal which is used to reject time-varying disturbances. The adaptive flutter suppression control is to achieve a stable reference model that represents the closed-loop dynamics as follows:

$$\ddot{w}_m + 2\zeta_m\omega_m\dot{w}_m + \omega_m^2 w_m = 0 \tag{55}$$

while the real plant is represented by

$$\ddot{w} + 2\zeta\omega_f\dot{w} + \omega_f^2 w = c_1\ddot{\delta} + c_2\dot{\delta} + c_3\delta + v(t) \tag{56}$$

where $v(t)$ is a time-varying disturbance.

We reply on the separation principle of control and estimation to use the estimator model as if it is the true model for designing a controller. Then, upon substitution, we get

$$\left(1-\hat{c}_1 k_w\right)\ddot{w}+\left(2\hat{\zeta}_f\hat{\omega}_f-2\hat{c}_1\dot{k}_w-\hat{c}_2 k_w\right)\dot{w}+\left(\hat{\omega}_f^2-\hat{c}_1\ddot{k}_w-\hat{c}_2\dot{k}_w-\hat{c}_3 k_w\right)w=c_1\ddot{r}+c_2\dot{r}+c_3 r+v \tag{57}$$

Thus, the adaptive law for the feedback gain k_w is obtained as

$$\dot{k}_w=\frac{2\hat{\zeta}_f\hat{\omega}_f-2\zeta_m\omega_m+2\zeta_m\omega_m\hat{c}_1 k_w-\hat{c}_2 k_w}{2\hat{c}_1} \tag{58}$$

$\zeta_m\omega_m$ is chosen to be such that $2\zeta_m\omega_m\hat{c}_1-\hat{c}_2<0$ if $\hat{c}_1>0$ or $2\zeta_m\omega_m\hat{c}_1-\hat{c}_2>0$ if $\hat{c}_1<0$. Then, $k_w(t)$ tends to

$$\bar{k}_w=\frac{2\zeta_m\omega_m-2\hat{\zeta}_f\hat{\omega}_f}{2\zeta_m\omega_m\hat{c}_1-\hat{c}_2} \tag{59}$$

in the limit as $t\to\infty$.

This implies the damping ratio tends to

$$\bar{\hat{\zeta}}=\frac{\zeta_m\omega_m}{\hat{\omega}_f} \tag{60}$$

The command signal to cancel out the disturbance can be designed by constructing a disturbance estimator as

$$\dot{\hat{v}}=-\gamma_v\frac{\partial J}{\partial\tilde{v}}=-\gamma_v\epsilon \tag{61}$$

Then, the steady state command for disturbance cancellation is computed as

$$c_3 r=\hat{v} \tag{62}$$

Thus, the adaptive command signal could also be computed from the least-squares parameter estimation as

$$\dot{r}=-\gamma_r\epsilon \tag{63}$$

Example: Consider the previous example of an airfoil in pitch and plunge. We will consider an open-loop modal identification of the plunge mode by applying a swept sine excitation signal from 15 - 17 rad/sec.

$$\delta=\delta_0\sin\left[\left(\omega_1-\omega_0\right)\frac{t}{t_f}+\omega_0\right]t \tag{64}$$

The plant modeling error ϵ is computed from the estimator model and the accelerometer output located on the airfoil. The top of figure 6 shows the plot of the estimated frequency of the plunge mode. The adaptation rates are chosen to be $\gamma_\omega=200$ and $\gamma_\zeta=1$. The plant corresponds to a natural frequency of $\omega_f=15.908$ rad/sec and a damping ratio of $\zeta=0.0036$. It can be seen that the estimated frequency approximates the true frequency of the plunge mode very well.

The lower plot of figure 6 is shows the estimated damping. The signal is noisy as expected because the true value is a very small number. Nonetheless, one can compute a mean value of about 0.0035 between 12 sec and 20 sec. This also agrees well with the true value.

Figure 7 is the plot of the estimated output from the estimator model and the true output. The estimated output converges to the true output after about 8 sec.

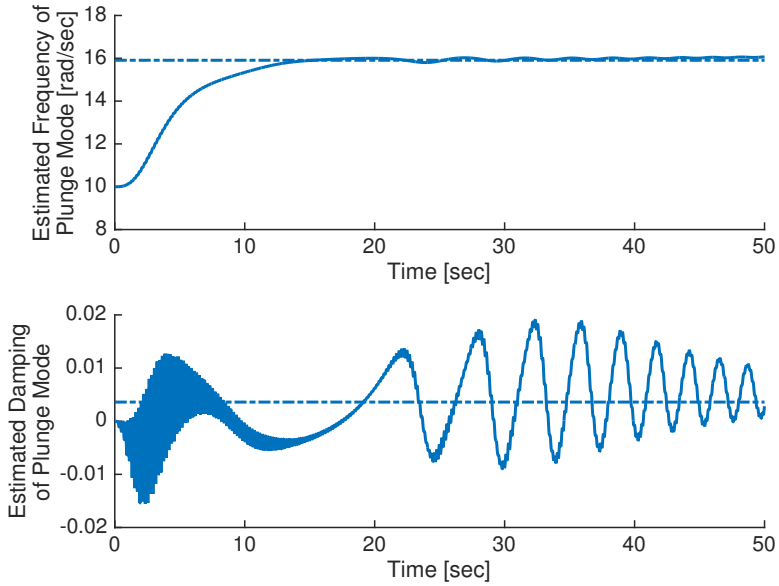

Figure 6. Estimated Frequency and Damping of Plunge Mode with Least-Squares. Swept sine wave from 15-17 rad/sec.

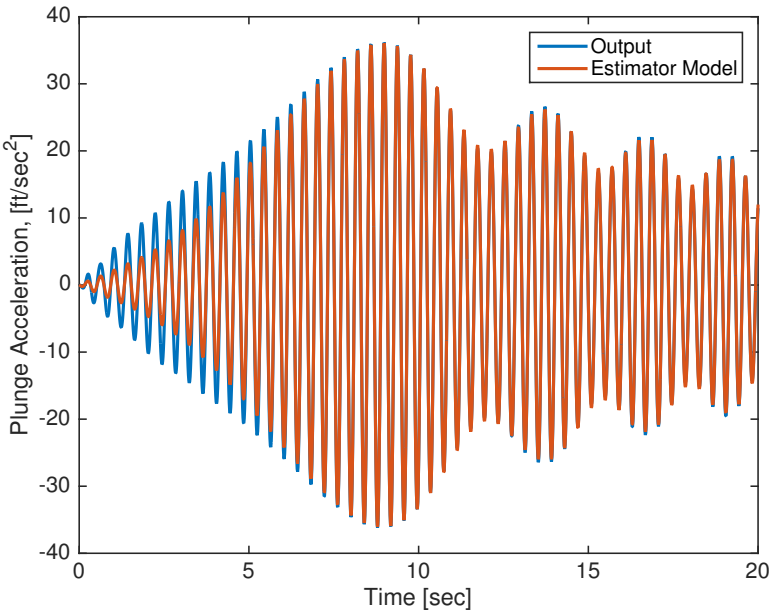

Figure 7. Estimated Output of Plunge Mode with Least-Squares

One difficulty with this approach is the sensitivity to the excitation signal. For example, if less is known about the parameter, and a broader sine excitation signal that varies in frequency from 10 - 20 rad/sec is used, the parameter estimates can wander away from their true values as shown in figure 8 below.

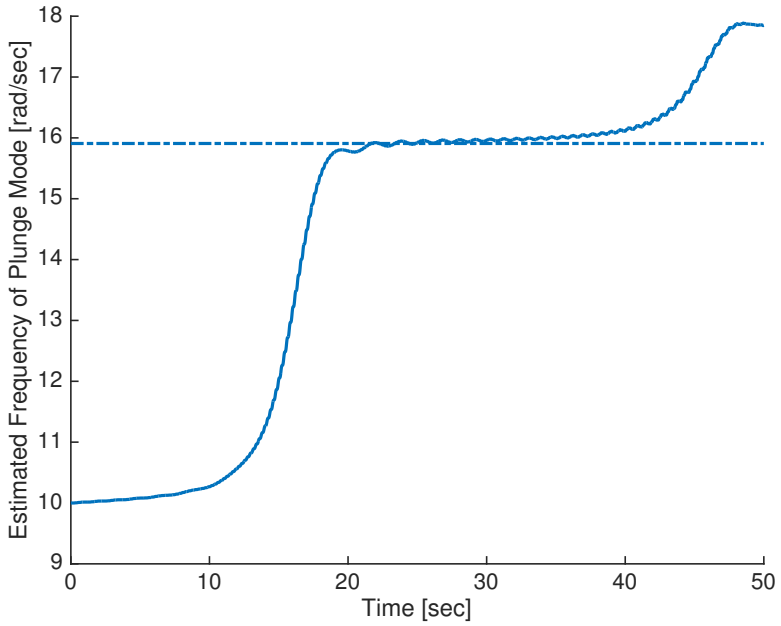

Figure 8. Estimated Frequency of Plunge Mode with Least-Squares. Swept sine wave from 10-20 rad/sec.

Next, in an attempt to compactly excite a broader range of frequencies, a 2 Hz square wave is used as the excitation signal δ. For $\dot{\delta}$, a signed Kronecker delta is used at the square wave axis crossings. γ_ω is set to 10. Lower frequency square waves (below 10 Hz) produced the best results, and higher amplitudes decreased convergence time more stably than increasing γ_ω as shown in figure 9 below.

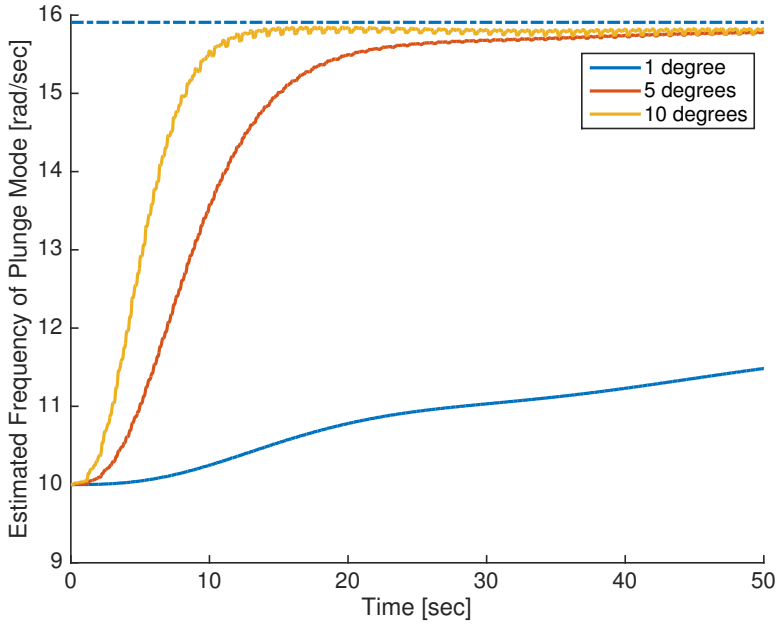

Figure 9. Estimated Frequency of Plunge Mode with Least-Squares. Various square wave amplitudes at 2 Hz

FIgure 10 shows that one downside to this method is that the estimated plunge mode damping is even noisier than before.

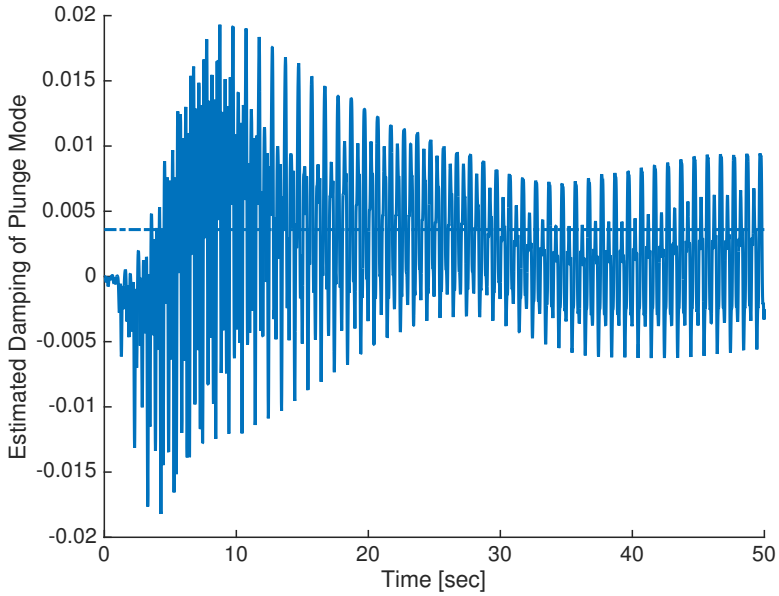

Figure 10. Estimated Damping of Plunge Mode with Least-Squares. 5 degree square wave at 2 Hz

Finally, random Gaussian noise is used to excite this Least-Squares adaptive system. Using adaption rates of $\gamma_\omega = 1000$ and $\gamma_\zeta = 1$, and a 10 Hz signal with zero mean and one degree standard deviation, both paramerts are shown to converge within the neighborhood of their true values in figure 11 below. However both remain noisy for obvious reasons.

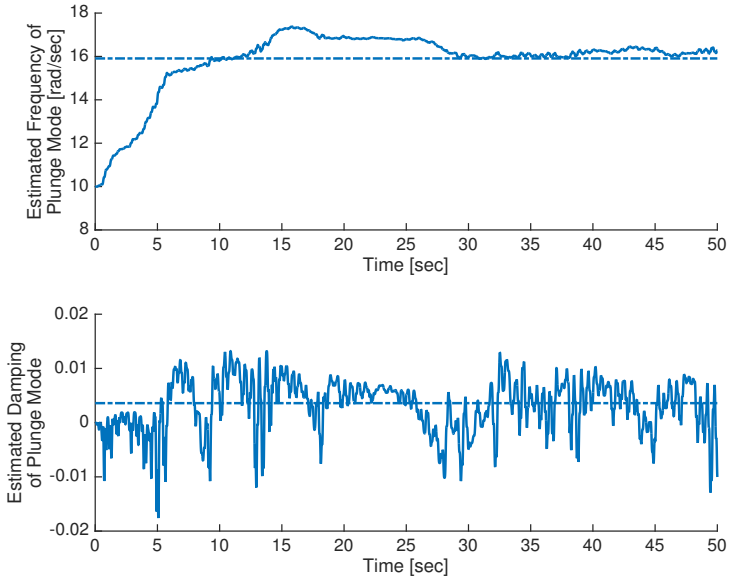

Figure 11. Estimated Frequency and Damping of Plunge Mode with Least-Squares. Gaussian noise with zero mean, one degree of standard deviation at 2 Hz

Because of the signal-to-noise ratio for the parameter estimation of the damping ratio, the recursive least-squares method is used where the adaptation rate γ_ω and γ_ζ are modified as follows:

$$\dot{\gamma}_\omega = -\eta_\omega \gamma_\omega^2 w^2 \tag{65}$$

$$\dot{\gamma}_\zeta = -\eta_\zeta \gamma_\zeta^2 \dot{w}^2 \tag{66}$$

where $\eta_\omega > 0$ and $\eta_\zeta > 0$ are the tuning parameters, chosen to be 0.5.

The plots in figure 12 show the estimated frequency and damping of the plunge mode generated by the Recursive Least-Squares method using the same excitation signal and initial adaption rates of those used in figure 6. The estimated frequency converges to a value of 15.933 rad/sec versus the true value of 15.908 rad/sec. This is an excellent agreement. The damping value also trends toward convergence with the final mean value of 0.0044 versus the true value of 0.0036. Compared to the results of figure 6, both the estimated frequency and damping stay within a tighter bound and exhibit less noise.

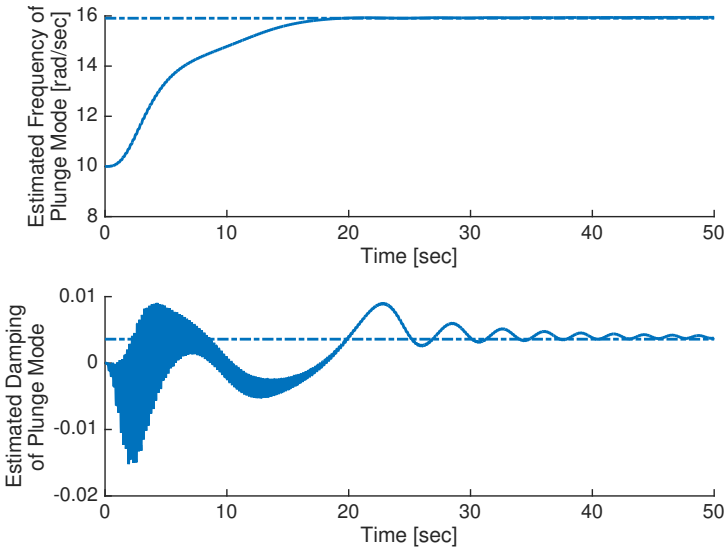

Figure 12. Estimated Frequency and Damping of Plunge Mode with Recursive Least-Squares

IV. Conclusions

This paper presents a modal identification approach to estimate the frequency and damping of a flutter mode of an aeroelastic system. The parameter estimation is based on the least-squares method using the output error. An application for an airfoil flutter is studied. The method shows that the parameter estimation is highly effective in modal identification of an aeroelastic system. In particular, the recursive least-squares demonstrates to be more effective than the standard least-squares gradient method in suppressing noise for signals with low signal-to-noise ratio. Using the adaptive parameter estimates, a flutter suppression can be designed to stabilized a flutter mode using the separation principle of control and estimation. In future work, we will develop flutter suppression control based on the modal identification method as presented in this paper.

References

[1]Nguyen, N., "Elastically Shaped Future Air Vehicle Concept," NASA Innovation Fund Award 2010 Report, October 2010, Submitted to NASA Innovative Partnerships Program, http://ntrs.nasa.gov/archive/nasa/casi.ntrs.nasa.gov/20110023698.pdf.

[2]Nguyen, N., Trinh, K., Reynolds, K., Kless, J., Aftosmis, M., Urnes, J., and Ippolito, C., "Elastically Shaped Wing Optimization and Aircraft Concept for Improved Cruise Efficiency," 51st AIAA Aerospace Sciences Meeting, AIAA-2013-0141, January 2013.

[3]Urnes, J., Nguyen, N., Ippolito, C., Totah, J., Trinh, K., and Ting, E., "A Mission Adaptive Variable Camber Flap Control System to Optimize High Lift and Cruise Lift to Drag Ratios of Future N+3 Transport Aircraft," 51st AIAA Aerospace Sciences Meeting, AIAA-2013-0214, January 2013.

[4]Nguyen, N. and Urnes, J., "Aeroelastic Modeling of Elastically Shaped Aircraft Concept via Wing Shaping Control for Drag Reduction," AIAA Atmospheric Flight Mechanics Conference, AIAA-2012-4642, August 2012.

[5]Nguyen, N., Ting, E., Nguyen, D., and Trinh, K., "Flutter Analysis of Mission-Adaptive Wing with Variable Camber Continuous Trailing Edge Flap," 55th AIAA/ASME/ASCE/AHS/ASC Structures, Structural Dynamics, and Materials Conference, AIAA-2014-0839, January 2014.

[6]Nguyen, N., Swei, S., and Ting, E., "Adaptive Linear Quadratic Gaussian Optimal Control Modification for Flutter Suppression of Adaptive Wing," AIAA Infotech@Aerospace Conference, AIAA 2015-0118, January 2015.

[7]Nguyen, N., "Least-Squares Model Reference Adaptive Control with Chebyshev Orthogonal Polynomial Approximation," AIAA Journal of Aerospace Information Systems, Vol. 10, No. 6, pp. 268-286, June 2013.